Modeling the Gas-Phase Reduction of Nitrobenzene to Nitrosobenzene by Iron Monoxide: A Density Functional Theory Study

Igor Zilberberg

Boreskov Institute of Catalysis, Novosibirsk 630090, Russia

Mykola Ilchenko

Institute of Cell Biology and Genetic Engineering, NAS of Ukraine, pr. Zabolotnogo, 148, Kiev 03143, Ukraine

Olexandr Isayev, Leonid Gorb, and Jerzy Leszczynski*

Computational Center for Molecular Structure and Interaction, Department of Chemistry, Jackson State University, Jackson, Mississippi 39217-0510

Received: November 4, 2003; In Final Form: March 13, 2004

The gas-phase selective reduction of nitrobenzene (NB) to nitrosobenzene (NSB) by iron monoxide has been for the first time studied by means of density functional theory (DFT) using both the hybrid and pure exchange-correlation functionals. As shown at both DFT levels, when interacting with NB, the iron center donates an electron into the nitro group to form the NB^- anion radical strongly coupled by FeO^+. This electron-transfer characteristic of the $NB^- - FeO^+$ intermediate reveals itself in the $\mathbf{S}^2$ operator expectation value that exceeds its eigenvalue of $S(S+1)$ by almost 1.0. Further reaction steps necessary to obtain nitrosobenzene from this intermediate are discussed. One of the possible steps based on the abstraction of oxygen from the nitro group by a ferrous center is considered in detail. This reaction appears to be favorable at the pure DFT level, whereas the hybrid theory predicts small endothermicity for the process.

1. Introduction

Selective reduction of nitrobenzene (NB) to nitrosobenzene (NSB) by ferrous iron has relevance to many areas. One application of this reaction is related to the synthesis from nitrosobenzene of various industrial products such as antioxidants, insecticides and photolacquers.[1] Transition metals and particularly iron oxides are known to exhibit catalytic activity in this process.[2] Another application concerns the deactivation of explosives by nontoxic materials and the remediation of nitroaromatic compounds (NAC) which are widely spread environmental contaminants. The various forms of ferrous iron complexed with both organic and mineral surfaces can be effectively used for the reduction of nitrobenzene to aminobenzene under anaerobic conditions.[3]

To our knowledge the reduction of NB to NSB by ferrous iron has not been studied by means of quantum chemical methods. The abundance of various iron oxides showing activity in the reduction of NB in different media and the lack of experimental data concerning the structure of the active center doenot allow one to address directly open questions concerning the detailed mechanism of this process by particular Fe(II)-contained systems. In this work an extremely simplified model of ferrous iron (iron monoxide) in the gas phase has been chosen in order to get some insight into the common features of the mechanism determined by the electron structure of Fe(II). It is also assumed that NB is reduced to NSB by ferrous iron via the direct removal of oxygen from the NO_2 group. Therefore, the removal of oxygen from NB by Fe(II) is theoretically studied in the present work using the following model reaction.

$$C_6H_5NO_2 + FeO \rightarrow C_6H_5NO + FeO_2 \qquad (1)$$

Modeling of the transition-metal compounds is well-known to be the most challenging task for quantum chemistry because of the number of theoretical and computational problems associated in particular with the open-shell electron structure of these systems.[4,5] A number of studies of iron-containing species has been recently carried out within density functional theory (DFT) using both the "pure" exchange-correlation and the hybrid functionals, including a fraction of the nonlocal Hartree−Fock exchange. These studies appear to be quite successful in energetic predictions despite all known limitations of this theory for such compounds. These limitations include improper treatment of spatially degenerate states, the abundance of local minima, and an absence of a systematic way of improving accuracy. Glukhovtsev et al., for instance, concluded that the hybrid three-parameter Becke's functional having a fraction of the pure Hartree−Fock exchange (B3LYP)[6] is capable of providing reliable results for iron-containing molecules and ions.[7] They found in particular that for the FeO molecule the B3LYP dissociation energy agrees with experiment within 1.2 kcal/mol. Gutsev et al.[8] found good accuracy of the pure DFT method in predicting the adiabatic electron affinities for the FeO_n ($n \leq 4$) iron oxides as studied using the functional given by a combination of the Becke's exchange[9] and Perdew−Wangs' correlation gradient-corrected functionals (hereafter denoted as the BPW91 functional).[10] The same oxides plus Fe_2O, Fe_2O_2, and Fe_2O_4 have been investigated in the work of Chertihin and co-workers[11] within the pure Becke's exchange

* To whom correspondence should be addressed.

10.1021/jp037351v CCC: $27.50
Published on Web 05/11/2004

and Perdew's correlation functionals[12] (denoted as the BP functional) and the hybrid B3LYP functional. They found that B3LYP favored the higher spin states relative to the pure BP functional and that a match between the calculated and observed isotopic frequency ratios was required to assign the ground states as triplet FeO_2 and quintet $Fe(O_2)$. The B3LYP functional was also employed in the work of Kellogg and Irikura to characterize the relative energetics of the FeO_xH_y species.[13] They reported that B3LYP accuracy in the prediction of the heats of formation depends on the specific case and is the highest in the case of FeH, FeO, FeOH, FeO(OH), and $Fe(OH)_2$. As can be concluded from the results obtained in the aforementioned studies, the pure and hybrid functionals are similar in predicting the geometries and frequencies when compared with the same spin state. Differences appeared in predictions concerning the origin of the ground state: the pure functionals favor low-spin states while the hybrid methods favor the high-spin states.

Unfortunately, none of the aforementioned papers contains information concerning the spin contamination for the spin states of iron (hydro)oxides treated at various DFT levels. The expectation value of the S^2 operator cannot be directly determined within the DFT method due to its dependence on the second-order density matrix, which is not defined in this theory. Despite that, there is the possibility of evaluating $\langle S^2 \rangle$ using a one-determinant wave function constructed from spin-up and spin-down Kohn−Sham orbitals. This is analogous to the standard technique developed for the unrestricted Hartree−Fock method (UHF). The value of $\langle S^2 \rangle$ obtained in this approach is shown to have a diagnostic meaning allowing one to assess the spin contamination of the open-shell states as obtained by means of spin-unrestricted density functional theory (UDFT).[14] In the present work the $\langle S^2 \rangle$ value is found to be especially useful for identifying intermediates formed between the electron donor and acceptor of which the NB−FeO complex appears to be a particular case. For this complex the electron transfer from Fe(II) onto the nitro group results in an electron configuration containing unpaired spin-up and spin-down electrons occupying the orthogonal d_{x2-y2} orbital of iron and the π^* orbital of the nitro group, respectively. A corresponding unrestricted B3LYP solution is characterized by the $\langle S^2 \rangle$ value, which exceeds its exact eigenvalue of 6.0 for the quintet by about 1.0.

2. Details of Calculations

The gas-phase interaction of nitrobenzene with FeO is studied at the UDFT level using the hybrid B3LYP and gradient-corrected local-density functionals BLYP and BPW91. Since an isolated nitrobenzene is a closed-shell molecule and the FeO molecule has a $^5\Delta$ ground state, the electronic state of the formed intermediate was treated as a quintet assuming that the total spin of the system does not change during the reaction. The geometries of the local minima and transition states were optimized without symmetry restrictions (C_1 symmetry was assumed) by the gradient procedure.[15] The local minima and transition states were verified by frequency analysis. Some minima have also been checked for SCF instability to ensure that all obtained solutions are stable.

All calculations were carried out within the Gaussian-98 package.[16] The standard 6-311++G(d,p) basis set was employed for light atoms along with the Wachters−Hay[17,18] all-electron basis set for iron using the scaling factors of Raghavachari and Trucks,[19] supplemented by diffuse functions. The latter basis set for iron will be denoted as 6-311++G(d,p) below.

To gain insight into the mechanism of decomposition of the nitro group by ferrous iron, the charge and spin difference density is obtained for the complex formed between NB and FeO. The charge difference density $\Delta\rho(\mathbf{r})$ (or spin difference density $\Delta\rho^s(\mathbf{r})$) is defined as

$$\Delta\rho(\mathbf{r}) = \rho(\mathbf{r}) - \rho_{NB}(\mathbf{r}) - \rho_{FeO}(\mathbf{r})$$

where $\rho(\mathbf{r})$ is the density for the complex; $\rho_{NB}(\mathbf{r})$ is the density for NB calculated for the geometry of the NB moiety of the complex using the "complete" basis set, i.e., including functions for the FeO moiety of the complex. The $\rho_{FeO}(r)$ density for FeO is calculated similarly to that of NB. This approach is analogous to the counterpoise method,[20] which is widely used for the estimation of the basis set superposition error.

Visualization of the geometries, charge, and spin densities has been performed by means of the MOLDEN program.[21]

3. Results and Discussion

3.1. Structure of Reactants and Products. All bond lengths of nitro- and nitrosobenzene predicted by both variants of the DFT functionals are in perfect agreement with those determined experimentally by Domenicano et al.[22] (Table 1). The calculated dipole moment of NB is fairly close to its experimental value.[23]

Since it is important for a discussion of the molecular mechanism of the nitro group decomposition, the frontier Kohn−Sham orbitals of NB (hereafter denoted as molecular orbitals) obtained at the B3LYP/6-311++G(d,p) level are plotted in Figure 1. As can be seen, the highest occupied molecular orbital (HOMO) appears to be the π type orbital delocalized over the benzene ring (Figure 1a). The lowest unoccupied molecular orbital (LUMO) contains the antibonding π^* type combination of the p(N) and p(O) orbitals and the bonding combination of the p(N) and the p_π orbital of the neighboring carbon atom (Figure 1b). Due to this composition of LUMO, some elongation of the N−O bond and shortening of the N−C bond can be expected in the case of the electron transfer into the LUMO of NB. Therefore, in reductive modifications of the nitro group, the composition of the LUMO orbital seems to play a key role since it determines the electron-withdrawing ability of NB. To obtain the electron affinity (EA) of NB, the anion radical of nitrobenzene has also been calculated at all three DFT levels used in this work (Table 1). The EA values estimated as a difference between the total energies of NB^- and NB are 1.22, 1.10, and 3.94 eV at the B3LYP, BLYP, and BPW91 levels, respectively. The BLYP functional appears to agree the most with the laser photoelectron spectroscopy value of 1.000 ± 0.010 eV.[24]

The FeO molecule has been the subject of extensive theoretical investigations.[8,25−27] The ground state is commonly accepted to be $^5\Delta$ arising from the $9\sigma^1 4\pi^2\delta^3$ configuration. In the present work the same ground state was obtained using the B3LYP, BLYP, and BPW91 functionals (Table 2). The assignment of the spatial and spin symmetry to the $^5\Delta$ state of FeO treated within UDFT for $S_z = 2$ has been made for the following reasons. First, the value of $\langle S^2 \rangle$ obtained at various levels is fairly close to its eigenvalue of 6.0 for the quintet state. This means that the obtained spin state is in fact a pure quintet. Second, the δ-type Kohn−Sham orbitals are occupied by almost three electrons. As a result the Mulliken charge and spin−orbital densities appear to be unequal for two spatial components of the δ orbital. Therefore, the obtained state is broken symmetry, a fact which was not mentioned in the above-cited DFT studies of FeO. The diatomic constants obtained for this molecule are presented in Table 2. The BLYP-level-predicted bond length,

TABLE 1: Total and Zero-Point Energies along with the Dipole Moments and Selected Bond Lengths of Nitrobenzene, Nitrozobenzene, the Anion Radical of Nitrobenzene, and Oxygen Species As Revealed by DFT Using the 6-311++G(d,p) Basis Set

		energy, au			bond lengths,[a] Å			
molecule	potential	total	ZPE	dipole moment, D	C−C	C−H	N−O	N−C
$C_6H_5NO_2$	B3LYP	-436.874 73	0.102 53	4.91	1.393	1.083	1.225	1.480
	BLYP	-436.766 69	0.098 94	4.88	1.403	1.089	1.245	1.498
	BPW91	-436.843 46	0.099 67	4.76	1.399	1.090	1.236	1.489
	Exp.			4.22 ± 0.08[b]	1.399[c]	1.093	1.223	1.486
C_6H_5NO	B3LYP	-361.639 31	0.096 76	4.06	1.395	1.084	1.214	1.440
	BLYP	-361.531 23	0.093 52	4.24	1.405	1.090	1.235	1.455
	BPW91	-361.603 16	0.094 04	[4.13]	1.402	1.091	1.227	1.450
$C_6H_5NO_2^-$	B3LYP	-436.919 38	0.099 26					
	BLYP	-436.806 94	0.095 60					
	BPW91	-436.885 06	0.096 36					
O ($S_z = 1$)	B3LYP	-75.089 88						
	BLYP	-75.079 27						
	BPW91	-75.076 85						
O^- ($S_z = 1/2$)	B3LYP	-75.149 01						
	BLYP	-75.142 08						
	BPW91	-75.136 76						
O_2 ($S_z = 1$)	B3LYP	-150.370 42	0.003 72					
	BLYP	-150.369 26	0.003 38					
	BPW91	-150.367 73	0.003 51					

[a] Bond lengths are averaged. [b] Experimental data from ref 23. [c] Electron diffraction data for the gas phase (ref 22).

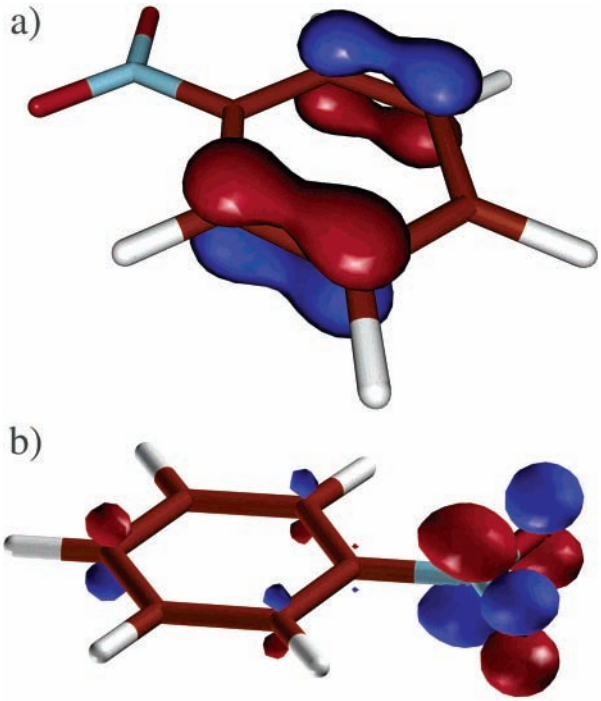

Figure 1. Highest occupied (a) and lowest unoccupied (b) orbital of nitrobenzene as predicted at the B3LYP/6-311++G(d,p) level.

vibrational frequency, and dipole moment for FeO appears to be close to the experimental data.[23,28,29]

The FeO_2 molecule has been studied by infrared spectroscopy[30] and the DFT method.[8,11,13,30,31] There is still controversy concerning the ground state of this molecule. The calculations of Andrews and co-workers at the B3LYP level using the [8s4p3d]-contracted Wachters basis set for iron and the 6-311+G(d,p) basis set for oxygen indicate that the ground state is $^5B_2$ with the first excited state $^3B_1$ being 2.42 kcal/mol higher in energy.[30] In the other paper the same group reported calculations using the nonhybrid DFT scheme with Becke's exchange and Perdew's correlation functional. At this so-called BP level with the same basis set as in the previous paper, the triplet state was predicted to be the lowest one with the quintet at 2.35 kcal/mol higher.[11] Plane and Rollason obtained the ground state $^5B_2$ at the B3LYP/6-311G level with the triplet $^3A_1$ as the lowest excited state, being 5.7 kcal/mol higher in energy.[31] Kellogg and Irikura predicted the same ground state and first excited state $^3B_1$ for the C_{2v} geometry using the B3LYP functional and the Stuttgart effective core potential.[13] The excitation energy was revealed to be about 1.4 kcal/mol. The calculations of Gutsev et al. at the BPW91/6-311+G(d) level yielded the triplet ground state $^3B_1$ with $^3A_1$ and $^5B_2$ being 0.7 kcal/mol higher.[8] Our calculations at the B3LYP and BLYP/6-311++G(d,p) levels agree completely with the results described above in that the hybrid functional B3LYP predicts quintet $^5B_2$ to be the ground state with quasi degenerate triplets $^3B_1$ and $^3A_1$ being 2.5 kcal/mol higher (Table 2). The nonhybrid functional BLYP yields a reverse ordering of the states. The ground state is $^3B_1$ with $^3A_1$ being very close in energy (0.6 kcal/mol) and $^5B_2$ being 2.7 kcal/mol higher. The spin contamination for these states is rather modest, as seen from Table 2.

The ordering of electronic states for FeO_2 can be qualitatively described if one assumes that there are four unpaired electrons distributed in five d orbitals of Fe^{4+} in the field of two O^{2-} anions (Chart 1). According to simple electrostatic reasons, the d orbitals can be ordered by energy as follows

$$e(d_{xy}) < \epsilon(d_{x2-y2}) < \epsilon(d_{xz}) < \epsilon(d_{xz}) < \epsilon(d_{z2}) < \epsilon(d_{yz})$$

For maximal spin $S = 2$, the electron configuration of Fe^{4+} is $(d_{xy}d_{x2-y2}d_{xz}d_{z2})$ or $(a_2a_1b_1a_1)$ in terms of the molecular orbitals. This configuration determines the many-electron state $^5B_2$ which seems to be the ground state in accordance with Hund's rule, assuming that d orbitals are quasi degenerate. Triplets arise from configurations with one pair of coupled electrons. It seems to be obvious that the lowest triplet would correspond to the pairing of electrons from the a_1 highest orbital and the a_2 lowest orbital to form the $(a_2^2a_1b_1)$ configuration. This configuration corresponds to the $^3B_1$ state. The next triplet $^3A_1$ arises from the $(a_2^2a_1b_1)$ configuration. For these reasons the ordering of the three lowest states of FeO_2 seems to be the following.

$$^5B_2 < ^3B_1 < ^3A_1$$

TABLE 2: Total Energies (E_{tot}), Zero-Point Energy (ZPE), $\langle S^2 \rangle$, Vibrational Frequencies (ω), Bond Lengths, and Dipole Moments for Iron Oxide Species As Obtained at the DFT Level Using Various Exchange-Correlation Potentials and the 6-311++G(d,p) Basis Set

molecule	potential	E_{tot}, au	ZPE, au	$\langle S^2 \rangle$	ω, cm^{-1}	Fe−O, Å	dipole moment, D
FeO ($^5\Delta$)	B3LYP	−1338.898 38	0.00204	6.035	896	1.61	5.27
	BLYP	−1338.955 66	0.00201	6.014	881	1.62	4.44
	BPW91	−1339.017 43	0.00207	6.017	907	1.61	4.38
	Exp				880a	1.62b	4.7 (0.2c
FeO^+ ($^6\Sigma^+$)	B3LYP	−1338.572 76	0.00187	8.768	819	1.64	4.92
	BLYP	−1338.628 65	0.00187	8.750	823	1.65	4.44
	BPW91	−1338.691 33	0.00193	8.757	847	1.64	4.47
FeO_2 ($^5B_2$)	B3LYP	−1414.125 59	0.00458	6.056	288,915,953	1.61,117.5	4.04
	BLYP	−1414.209 57	0.00475	6.025	288,874,911	1.63,117.3	3.45
	BPW91	−1414.268 97	0.00485	6.025	294,896,936	1.61,117.2	3.37
FeO_2 ($^3B_1$)	B3LYP	−1414.121 58	0.00491	2.127	186,883,940	1.58,142.2	2.21
	BLYP	−1414.213 90	0.00472	2.034	193,891,1001	1.60,137.8	2.11
	BPW91	−1414.270 78	0.00485	2.037	198,911,1019	1.59,137.7	2.03
Fe ($S^z = 2$)	B3LYP	−1263.650 24 ($4s^{1.80}3d^{6.194}d^{0.01}$)[d]		6.010			
	BLYP	−1263.684 57 ($4s^{1.463}d^{6.534}d^{0.01}$)		6.008			
	BPW91	−1263.745 20 ($4s^{1.31}3d^{6.68}4d^{0.01}$)		6.007			

[a] Reference 28. [b] Reference 23. [c] Reference 29. [d] Natural electron configuration of as revealed by the NBO analysis.[41]

CHART 1: Lowest States of FeO_2 As Predicted Assuming the Fe(+4) and O(−2) Oxidation States

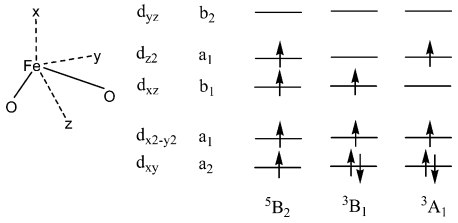

This ordering is in accord with the B3LYP predictions. One can, however, anticipate competition between $^5B_2$ and $^3B_1$ depending on the splitting of the d shell at the iron center due to the bent OFeO structure. The larger the splitting, the smaller is the gap between the quintet and triplet. To address the problem described above, a detailed study of the electronic structure of FeO_2 using both the DFT and the complete active space self-consistent field (CASSCF) approach will be presented elsewhere.

Considering two different classes of the DFT method, one can clearly see that quasi degeneracy of the d orbitals (and, therefore, closeness of the quintet and triplets) is responsible for inconsistent predictions of these methods for the quintet and triplet states of FeO_2. The proportion of the correlation and exchange in the particular functional determines whether the higher or lower spin state is the lowest one. The B3LYP method seems to favor the quintet because the Hartree−Fock exchange account leads to the prevalence of the exchange over the correlation in the correlation-exchange potential. Otherwise due to the underestimation of the exchange, the nonhybrid DFT methods seem to favor the lower spin configurations with paired electrons.

3.2. Structure of the FeO−Nitrobenzene Complex. The results of our calculations reveal that FeO interacts with nitrobenzene to form an almost planar intermediate shown in Figure 2a. The nonplanarity is caused by the iron oxide oxygen center located slightly out-of-plane, formed by NB and the iron atom. Analyzing the geometrical data presented in Table 3 one may see that there is similarity in the geometrical parameters predicted by DFT using various functionals. In particular, all functionals predict some elongation of the N−O and the Fe−O bonds of iron monoxide and some shortening of the bond between the nitro group and the aromatic ring upon formation of the NB−FeO complex. This is perfect verification of the

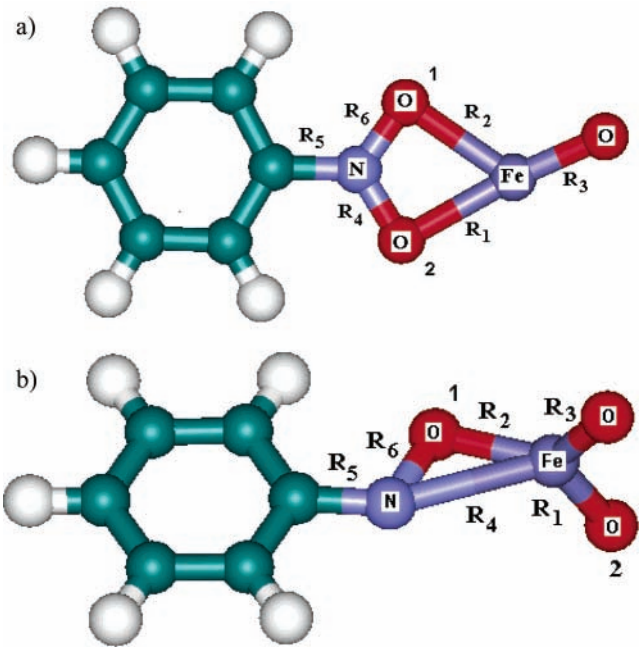

Figure 2. Intermediate formed due to the interaction between nitrobenzene and iron monoxide (a) and between nitrosobenzene and iron dioxide (b) as obtained at the B3LYP/6-311++G(d,p) level.

aforementioned qualitative predictions concerning the electron transfer from FeO into the nitro group. Exactly the same effect of electron transfer on the NB structure resulting in the elongation of the N−O bonds was obtained previously in our semiempirical study of the reduction of nitrobenzene by zero-valence iron.[32]

Evidence of the electron transfer from ferrous center into NB is provided by nonzero Mulliken atomic spin densities for the NB moiety in the NB−FeO complex (Chart 2). Taking into account that isolated nitrobenzene molecule has closed-shell electron configuration with zero total spin, these spin densities which add up to 0.85 au for the NB moiety (at the B3LYP level) can be considered as a result of the electron transfer from the ferrous center into NB. Pure functionals do not reveal such a profound effect, predicting transfer of only 0.13 au (see BLYP densities in Chart 2, where we did not report the BPW91 densities since they are fairly close to those of BLYP).

Taking into account well-known shortcomings of Mulliken population analysis that, in particular, result in a quite arbitrary

TABLE 3: Selected Geometrical Parameters for NB−FeO (I), the Transition State (TS), and the NS−FeO_2 Complex (F) As Predicted by Various Functionals Using the 6-311++G(d,p) Basis Set

	structure	R_1[a]	R_2	R_3	R_4	R_5	R_6	A_1[b]	A_2	A_3	D_1	D_2	D_3
B3LYP	I	2.06	2.06	1.65	1.31	1.39	1.31	150.6	64.5	113.6	180.0	180.0	180.0
	TS	1.71	1.88	1.63	2.41	1.41	1.35	155.8	84.1	50.8	170.5	−114.6	106.4
	F	1.62	1.99	1.62	2.88	1.39	1.26	134.8	111.6	41.7	−86.2	157.0	167.0
BLYP	I	2.10	2.19	1.66	1.32	1.41	1.29	116.6	61.6	114.5	180.0	180.0	180.0
	TS	1.76	1.90	1.64	1.78	1.43	1.38	126.6	81.8	89.34	124.4	−108.8	112.9
	F	1.62	1.81	1.62	2.59	1.38	1.35	122.4	120.3	52.1	−91.9	174.4	156.2
BPW91	I	2.08	2.16	1.65	1.31	1.41	1.28	115.6	61.7	114.7	180.0	180.0	180.0
	TS	1.73	1.89	1.63	1.83	1.42	1.36	124.6	82.3	87.8	122.3	−108.9	112.8
	F	1.61	1.83	1.61	2.25	1.37	1.35	121.9	121.8	66.7	−90.0	180.0	152.9

[a] Listed in the table distances are shown in Figure 2. [b] The following designations are used for valence and dihedral angles: A_1 = <$OFeO_1$, A_2 = <O_1FeO_2, A_3 = <O_1NO_2; D_1 = <$OFeO_1N$, D_2 = <FeO_1NC_3, and D_3 = <$O_2NO_1C_3$.

CHART 2: Mulliken Spin Densities on Atoms of NB−FeO and FeO As Obtained at the B3LYP and BLYP/6-311++G(d,p) Levels

B3LYP

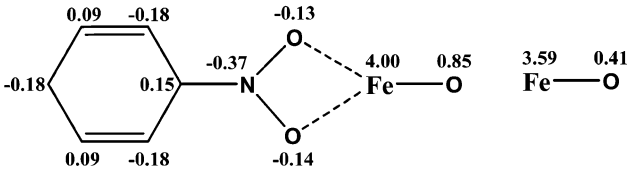

BLYP

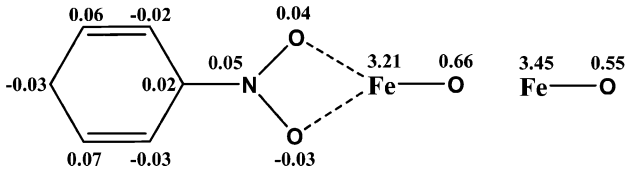

partition of the charge and spin density between neighboring atomic centers, the question of the electron-transfer nature of the ground state of NB−FeO was also considered using charge ($\rho(\mathbf{r})$) and spin density function ($\rho^s(\mathbf{r})$) for the whole complex. As can be seen from the plot of $\Delta\rho(\mathbf{r})$ (Figure 3a) and $\Delta\rho^s(\mathbf{r})$ (Figure 3b) obtained on the base of the B3LYP/6-311++G(d,p) data, there are correlated redistributions of the charge and spin densities between NB and FeO due to the intermolecular interaction. There is a transfer of the β-spin density from FeO (shown in red in Figure 3b) into the nitro group of NB and the benzene ring. This shift of spin-down density is accompanied by the appearance of the α-spin density on iron monoxide. There is also the redistribution of charge between FeO and the nitro group moiety of the NB−FeO complex (Figure 3b) due to the charge transfer from FeO toward NB. The difference spin density provides us also with information concerning the orbitals that are involved in the spin transfer. As can be clearly seen from Figure 3b, these are the π^* orbital of the nitro group and antibonding combination of the d_{x2-y2}(Fe) and s(O) orbitals. The resultant electron configuration of NB−FeO contains the α electron localized on the FeO moiety and the β electron localized on the nitro group in addition to four α electrons of the d shell of the iron center.

In addition to the considered-above redistribution of the electron density, additional evidence of the electron transfer in question is provided by the mean value of the S^2 operator. At the B3LYP/6-311++G(d,p) level the $\langle S^2\rangle$ appears to be almost 1.0 larger than its eigenvalue of $S(S+1) = 6.0$ (Table 4). Pure functionals BLYP and BPW91 induced a lower spin contamination (Table 4), which seems to be a consequence of the

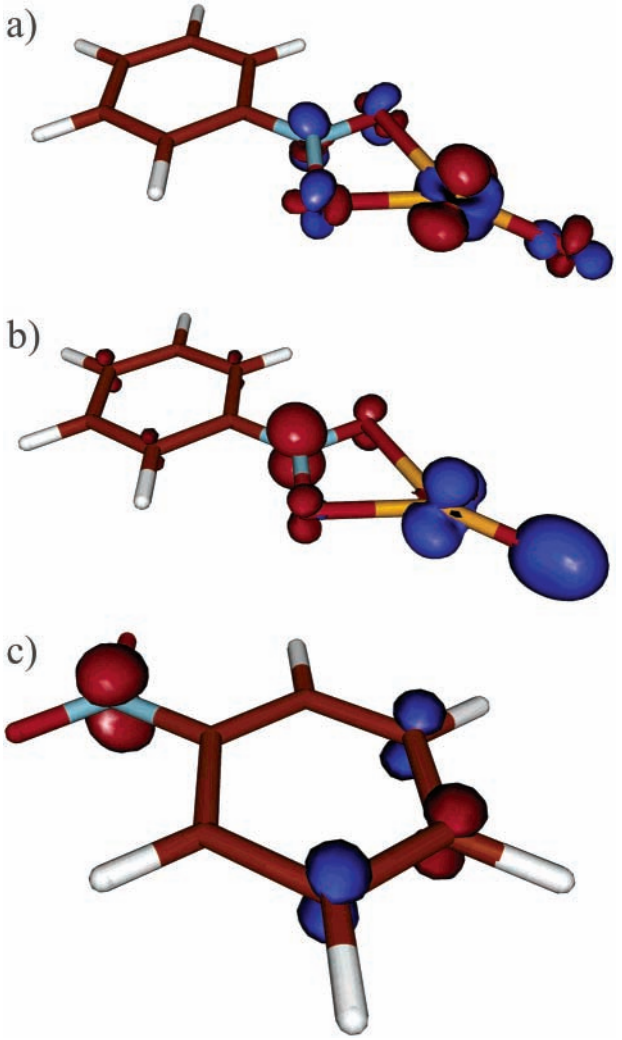

Figure 3. Difference charge (a) and spin (b) densities as obtained at the B3LYP/6-311++G(d,p) level along with the spin density of the excited $^1B_2$ state (c) of nitrobenzene obtained by using the broken-symmetry unrestricted B3LYP solution.

underestimation of the exchange effects in comparison with B3LYP (containing an admixture of the exact Hartree−Fock exchange potential) and is observed also for other molecules.[33] In some sense the obtained spin state is analogous to the broken symmetry (BS) solution for the dissociated H_2 molecule which might be obtained within the unrestricted Hartree−Fock method as well as with any DFT method. The BS determinant for H_2 comprises the α and β molecular (or Kohn−Sham) orbitals localized on different nuclei, which is necessary to predict the correct dissociation limit of two H atoms. The $\langle S^2\rangle$ value for such a determinant is exactly 1.0 in the dissociation limit,

TABLE 4: Total Energy ($E_{tot.}$), Zero-Point Energy (ZPE), and $\langle S^2\rangle$ for the NB−FeO Complex (I), the Transition-State Complex (TS), and the NS−FeO_2 (F) Complex along with the Activation Energy ($E^{\ddagger}$) for Oxygen Transfer from the Nitro Group into FeO

exchange correlation potential	$E_{tot.}$,[a] au; ZPE, au; $\langle S^2\rangle$					$E^{\ddagger}$, kcal/mol; ZPE-corrected $E^{\ddagger}$, kcal/mol	
	I ($S_z = 2$)	I ($S_z = 3$)	I (projected quintet)	TS	F ($S_z = 2$)	before projection	after projection
B3LYP	−0.828 49	−0.770 84	−0.838 89	−0.77 330	−0.795 79	34.6	41.2
	0.103 64			0.102 74	0.102 78	34.1	
	6.917 (6.032)[b]	12.030		6.083	6.104		
BLYP	−0.776 07	−0.755 94	−0.777 52	−0.750 31	−0.787 54	16.2	16.8
	0.101 16			0.099 02	0.099 20	14.8	
	6.404 (6.004)	12.017		6.034	6.037		
BPW91	−0.914 88	−0.895 44	−0.916 34	−0.882 34	−0.919 44	20.4	21.0
	0.101 85			0.099 78	0.100 27	19.1	
	6.420 (6.004)	12.017		6.035	6.039		

[a] Total energies are given with respect to −1775.0 au. [b] The $\langle S^2\rangle$ value after annihilation of the septet.

indicating that this determinant is a 50−50 mixture of the pure singlet and triplet two-determinant functions.

The spin states just described for NB−FeO and H_2 are examples of an unrestricted Hartree−Fock or DFT solution characterized by

$$\langle S^2\rangle = S(S+1) + m \qquad m = 1, 2, ...$$

One can show[34] that the corresponding unrestricted determinant must be of the following form

$$|(\text{paired orbitals})\ (\text{unpaired orbitals})\ a_1\alpha,...,a_m\alpha, b_1\beta,..., b_m\beta\rangle$$

in which orbitals a_i and b_i ($i = 1, m$) have negligible overlaps, "paired orbitals" are those α and β spatial orbitals having overlaps close to 1.0, and "unpaired orbitals" denote α orbitals exactly orthogonal to each other and all occupied orbitals. Such a set of spatial orbitals can be referred to what is known as Löwdin's paired orbitals[35] obtained by unitary transformations of α and β sets. The deviation of $\langle S^2\rangle$ from its eigenvalue $S(S+1)$ for the considered unrestricted determinant is in fact determined by the number of β orbitals b_j ($j = 1, m$) which have negligible overlaps with corresponding α orbitals and, because of that, can be called unpaired β orbitals.

An interesting example of the unrestricted determinant of the above-considered form is given by UDFT studies of diiron−oxo proteins consisting of two paramagnetic $Fe^{3+}(d^5)$ centers bridged by a nominally diamagnetic oxo center.[36] An open-shell singlet state for this system, in which there are five spin-up electrons on one iron center and five spin-down electrons on another, is described by an unrestricted determinant having an $\langle S^2\rangle$ value of about 5.0.

For the NB−FeO intermediate after the annihilation of the first contaminant (septet), $\langle S^2\rangle$ becomes fairly close to its eigenvalue for the quintet (Table 4). One can conclude that in the Kohn−Sham determinant (Ψ^{KS}) there are no other substantial admixtures to the pure quintet state. Therefore, the latter can be fairly well approximated by the normalized sum of pure quintet and septet states.

$$\Psi^{KS} = c_S\Psi^S + c_{S+1}\Psi^{S+1}$$

In this expression the weight of the first contaminant (here septet) is

$$c_{S+1}{}^2 = (\langle S^2\rangle - S(S+1))/2(S+1)$$

$$c_S{}^2 = 1 - c_{S+1}{}^2$$

The energy of the Ψ^S state (in our case quintet) can be estimated from the following expression

$$E^S = (E^{KS} - c_{S+1}{}^2E^{S+1})/(1 - c_{S+1}{}^2) = E^{KS} + (E^{KS} - E^{S+1})c_{S+1}{}^2/c_S{}^2$$

in which E^{KS} denotes the energy of the contaminated state described by the Kohn−Sham determinant. In practice one can use this formula only when the pure septet energy is available. This is the case for the NB−FeO complex since its septet state appears to be a pure one for a good approximation as revealed by the B3LYP, BLYP, and BPW91 calculations (geometry optimized for the spin projection of $S_z = 2$) (Table 4). The energies of the quintet state estimated in this approach are given in Table 4 along with those for the septet. Since the septet is higher in energy than the quintet for all three potentials, the projected quintet appears to be lower than the contaminated state. However, the difference in energy between the "pure" and contaminated quintet is relatively small at about 0.01 au for B3LYP and 0.001 au for the BLYP and BPW91 level calculations.

To determine whether the redistributions described above of charge and spin can be attributed to a one-electron transfer (or, equivalently, β spin) from FeO into NB, the following "proof by contradiction" is used. If one suggests that the redistribution of electron density is not equivalent to the charge transfer, then this effect must be related to the spin and charge polarization within the NB moiety caused by the complexation to FeO. The excited states of nitrobenzene corresponding to the β-spin transfer from the occupied orbitals of NB have been calculated for $S_z = 0$ using the spin-polarized B3LYP approach. The obtained solution is of the BS type (as follows from $\langle S^2\rangle = 1.01$), and as well as in the NB−Fe case some spin density appears on the π^* orbital of the nitro group (Figure 3c). Unlike the case of the NB−FeO complex, the spin appearing in this orbital is singlet coupled with the spin of the other sign occupying the σ type orbitals on the oxygen atoms of the nitro group. Therefore, the initial suggestion of the spin polarization is wrong, and the obtained spin density shift from FeO into the nitro group is undoubtedly the result of a one-electron transfer from FeO to NB.

3.3. Mechanism of Nitrobenzene-to-Nitrosobenzene Reduction by FeO. Considering the mechanism of the overall reaction (1), the following thermochemical predictions have to be first put forward. Using the zero-point-corrected energies obtained for the NB, NS, FeO, and FeO_2 molecules, the heat of reaction (1) is estimated to be 3.1, −13.3, and −8.8 kcal/mol at the B3LYP, BLYP, and BPW91 levels, respectively (Table

TABLE 5: Heats of Gas-Phase Reactions (kcal/mol) Related to the Selective Reduction of Nitrobenzene by Iron Monoxide As Estimated from Zero-Point-Corrected DFT Results Using the 6-311++G(d,p) Basis Set

reaction	B3LYP	BLYP	BPW91	$\Delta_r H°_{gas}$ [a]
$C_6H_5-NO_2 \rightarrow C_6H_5-NO + O(S_z=1)$	87.7	94.6	99.0	91.2[a]
$Fe(S_z=2) + O(S_z=1) \rightarrow FeO\ (^5\Delta)$	−98.0	−119.1	−121.3	-96.8 ± 3[b]
				-93.1 ± 3[c]
				-95.8 ± 2[d]
$FeO\ (^5\Delta) + O(S_z=1) \rightarrow FeO_2(^5B_2)$	−84.6	−107.9	−107.9	-102.0 ± 5[b]
				-99.0 ± 6[c]
$C_6H_5\text{-}NO_2 + FeO\ (^5\Delta) \rightarrow C_6H_5\text{-}NO + FeO_2(^5B_2)$	3.1	−13.3	−24.1	−10.8[e]
$C_6H_5\text{-}NO_2 + FeO\ (^5\Delta) \rightarrow C_6H_5\text{-}NO_2^- + FeO^+$	174.2	177.8	175.1	
$2O(S_z=1) \rightarrow O_2(S_z=1)$	−117.3	−130.1	−132.1	-119.110 ± 0.024[a]

[a] Thermochemical data from ref 39. [b] Derived by Hildenbrand from studies of gaseous equilibria involving Fe, FeO, and FeO_2 species by means of high-temperature mass spectrometry.[40] [c] Mass spectrometric Knudsen effusion method.[42] [d] Mass spectrometric Knudsen cell method.[43] [e] Derived using Hildenbrand's data on $\Delta_r H°$ for FeO_2.

5). Thus this reaction is exothermic only at the pure DFT level. Such inconsistency of these methods seems to have the same origin as that considered above for the ordering of higher and lower spin states. Pure general-gradient-approximation (GGA) methods such as BLYP are known to suffer overbinding errors as high as 20 kcal/mol for non-transition-metal compounds.[37] The hybrid methods reduce substantially these errors due to exact-exchange mixing. The only problem is that the parameters of the hybrid functional such as B3LYP are obtained from the fit to the G2 atomization energies set.[38] That makes this functional dependent on this particular set of reference systems with no guarantee for securing reliable results for other species. That seems to be the case for iron dioxide.

Considering the available thermochemical data,[39] one can see (Table 5) that B3LYP underestimates both the (−NO)O and (OFe)O bond strengths, while BLYP and BPW91 systematically overestimates these values. At the BLYP and BPW91 level the Fe(II)−O bond strength agrees with the experimental value obtained by Hildenbrand[40] within the experimental uncertainty while the B3LYP-predicted D_0(OFe−O) is by 8.4 kcal/mol lower than the lowest limit of the experimental value obtained by Kaibicheva et al.[42] (Table 5). At the same time, B3LYP-predicted dissociation energy for FeO agrees with Hildebrand's and other experimental data within experimental uncertainty, while both pure functionals overestimate D_0(Fe−O) by more than 20 kcal/mol (Table 5). The question arises why B3LYP, showing excellent credibility in the case of FeO, disagrees with experiment in the case of FeO_2. In this regard it is worth noting that the calculated D_0(OFe−O) value is lower than D_0(Fe−O) by 11−13 kcal/mol at all DFT levels in contrast to the experimental trend of increasing Fe−O bond strength by 5−6 kcal/mol when going from FeO to FeO_2 (Table 5). A similar tendency was found for the cobalt oxides. The B3LYP calculations predicted bond strength decrease from 88.3 kcal/mol for D_0(Co−O) (experimental value, 87.6 kcal/mol) to 73.3 kcal/mol for D_0(OCo−O), respectively.[44] The DFT-predicted decrease of the bond dissociation energy in FeO_2 seems to result from some repulsion between Fe−O bonds in dioxide. If the experimental data are correct, one may suggest that an additional stabilization of FeO_2 arises from overestimated attraction between oxygen centers which counterbalances the repulsion between Fe−O bonds. This suggestion is in line with the results of Plane and Rollason who predicted the existence of a stable peroxo isomer of FeO_2 lying by 49.2 kcal/mol higher in energy than dioxo FeO_2 at the B3LYP/6-311G(d) level.[31] There is also a possibility of experimental errors, as was pointed out by Plane and Rollason.[31] To judge whether the only existing experimental values of D_0(OFe−O) obtained by Hildenbrand and Kaibicheva with coauthors are correct, additional experimental data must be obtained. As far as verification of theoretical predictions on iron oxides is concerned a higher theory level, e.g. the multiconfiguration self-consistent-field approach, is required to obtain alternative estimations of the iron oxide bond energies. Such approaches could also be helpful in addressing the problem of the interconnection between D_0(OFe−O) and D_0(Fe−O).

The intermolecular electron transfer from FeO and NB to form the ionized FeO^+ and NB^- species is predicted at all levels of DFT to be strongly thermodynamically forbidden (Table 5). This may be explained by the common situation when the electron affinity of an acceptor cannot compensate for the ionization potential of a donor which is usually larger in magnitude. Otherwise, the electron transfer between the FeO and NB moieties of the NB−FeO complex results in the formation of a quite stable intermediate whose structure can be drawn as $[(C_6H_5NO_2^-)^{\downarrow}\cdots^{\uparrow}(Fe^{3+}O)]$. Moreover, taking into account that no other states (like those without electron transfer) for the NB−FeO intermediate have been revealed by our DFT study, one can conclude that the interaction of FeO with the nitro group results in the nonbarrier transfer of one electron from ferrous iron into the nitro group. The obtained anion radical NB moiety would be apparently very reactive toward abstraction of hydrogen atoms from the hydrocarbons or protons from solution if they would be present in the media. For the gas-phase reaction considered in this work the reductive transformation of the nitro into the nitroso group is accessible only via formation of isolated O^- or the abstraction of the oxygen center from the nitro group to form FeO_2. Corresponding reactions are as follows.

$$C_6H_5-NO_2 + FeO \rightarrow (C_6H_5-NO_2^-)^{\downarrow}\cdots^{\uparrow}(Fe^{3+}O) \quad (2)$$

$$(C_6H_5-NO_2^-)^{\downarrow}\cdots^{\uparrow}(Fe^{3+}O) \rightarrow [C_6H_5-NO-FeO]^+ + O^- \quad (3)$$

$$(C_6H_5-NO_2^-)^{\downarrow}\cdots^{\uparrow}(Fe^{3+}O) \rightarrow C_6H_5-NO\ (^1A') + FeO_2 \quad (4)$$

The decomposition of the $-NO_2^-$ group complexed by the iron oxide to produce O^- (reaction 3) seems to be a thermodynamically unfavorable process because of the high energy of bonding between the −NO group and O^-. The latter is estimated from the calculated energies of NS and O^- (Table 1) to be about 82 kcal/mol. Therefore reaction 4 seems to be the major way of producing nitrosobenzene via iron monoxide when no other reactants (protons from water for instance) are involved in the process.

To estimate the activation energy of reaction 4, a transition-state (TS) search has been performed for this reaction. The geometrical structure of the obtained TS complex is displayed in Figure 4. The most important geometrical parameters predicted at various levels of DFT are listed in Table 3. The

TABLE 6: Relative Energies (kcal/mol) of the Whole Reaction FeO + NB → FeO_2 + NS As Predicted by Various Functionals Using the 6-311++G(d,p) Basis Set

	FeO + NB	FeO−NB	TS	FeO_2−NS	FeO_2 + NS
B3LYP	0.0	−34.8 (−35.3)[a]	−0.1 (−1.3)	−14.2 (−15.4)	5.2 (3.1)
BLYP	0.0	−33.7 (−33.6)	−17.5 (−18.8)	−40.9 (−42.0)	−11.6 (−13.3)
BPW91	0.0	−33.9 (−33.8)	−13.5 (−14.7)	−36.7 (−37.7)	−7.1 (−8.8)

[a] ZPE-corrected values in parentheses.

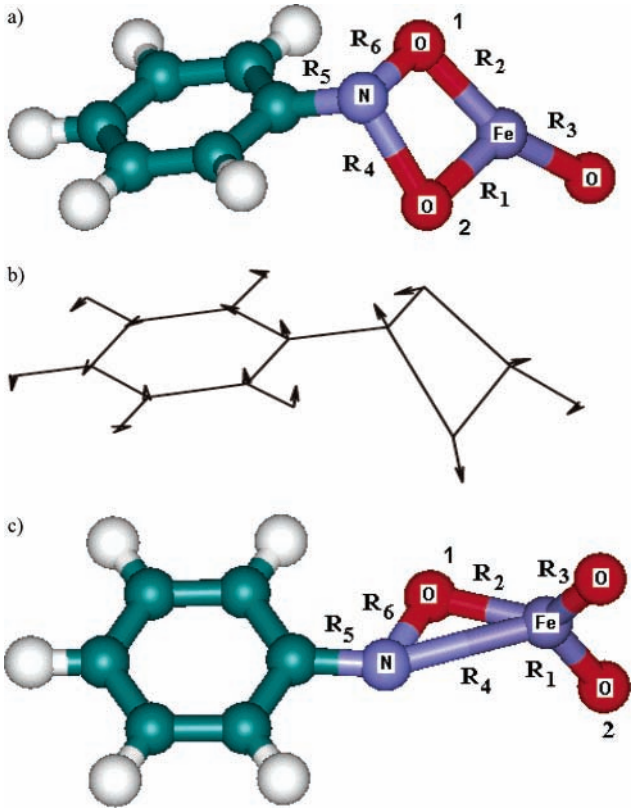

Figure 4. Structure of the transition state (a), the composition of the transition vector (b), and the structure of the reaction product (c) as obtained at the B3LYP/6-311++G(d,p) level.

TS complex has a nonplanar geometry with the O1, O2, and Fe atoms outside of the ring plane (Figure 4a). One may see that the structural parameters calculated at all considered levels are quite similar. To confirm that the obtained TS corresponds to reaction 4, the structure of the transition vector has been analyzed (see Figure 4b). One may see that the shape of it unambiguously suggests that the structure of the transition state is located properly. We have also used the structure of the transition vector to locate the product of the reaction of interest. To do that the geometry of the transition state was changed accordingly to the directions determined by the transition vector and then fully optimized. The structure of the product located in such a way is presented in Figure 4c. One may see that the product of the reaction is a bidentate complex of nitrosobenzene and FeO_2. The most important geometrical parameters are given in Table 3. Similarly, as noticed also for the geometrical parameters of the initial complex, the transition-state molecular parameters are just slightly different for various considered DFT methods. The activation energy corrected in accord with the projection used above of the contaminated quintet state is presented in Table 4. The lowest obtained activation energy of 16.8 kcal/mol is predicted at the BLYP level which seems to be the most reliable for studying the process under consideration. In addition in Chart 3 we have schematically presented the reaction path of FeO and NB interaction for all considered in the paper DFT functionals.

CHART 3: Reaction Path of FeO and NB Interaction as It Follows from B3LYP, BLYP, and BPW91 Calculations

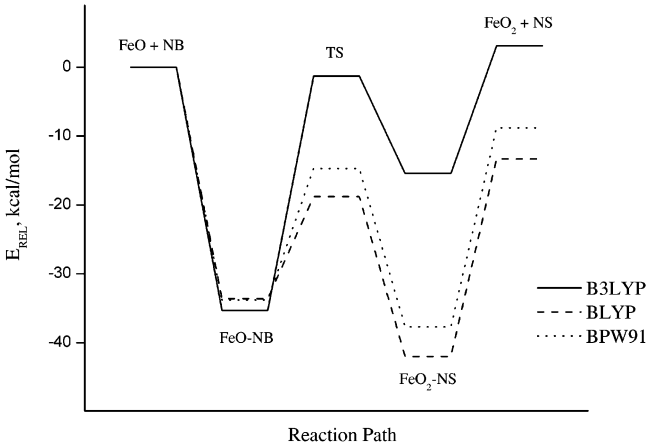

Unfortunately, to the best of our knowledge, there are no kinetics data on the gas-phase reaction of the ferrous center with nitroaromatics. However, the obtained activation energy appears to be much lower than the energy of bonding between NB and FeO estimated to be about 34 kcal/mol. This reason formally allows for reaction 1 to proceed at appropriate temperatures.

ZPE-corrected relative energies for the overall reaction are displayed in Table 6 and plotted as the energy profile (Chart 3). It turns out that the energy of interaction between nitrobenzene and iron monoxide (35.3, 33.6, and 33.8 kcal/mol for B3LYP, BLYP, and BPW91, respectively) is almost the same at all used DFT levels. At the same time, the interaction energy between nitrosobenzene and iron dioxide varies significantly for hybrid and pure functionals: 18.5 for B3LYP and 28.7, 28.9 for BLYP and BPW91, respectively. Such differences originate in fact from the discussed-above underestimation of the bond energy between FeO and O revealed by the hybrid DFT as compared with the pure DFT methods. The B3LYP-predicted value of D_0(OFe−O) appears to be less than D_0(NS−O), and it makes reaction 1 slightly endothermic (Table 6, Chart 3). The relatively low affinity of FeO to the oxygen atom predicted by B3LYP seems to be also responsible for a too-high activation barrier (34.1 kcal/mol) for the abstraction of oxygen from the nitro group, which appears to be comparable with the NB−FeO interaction energy.

4. Conclusions

The DFT study of the selective reduction of nitrobenzene to nitrosobenzene by iron monoxide in the gas phase using both the hybrid (B3LYP) and pure functionals (BLYP and BPW91) allows us to make the following conclusions.

The thermodynamics of the removal of oxygen from the nitro group by FeO to form FeO_2 is determined by the ability of ferrous iron to compensate for the energy necessary to brake the N−O bond by the formation of the oxo ferrous−iron bond. As follows from the thermochemical data, the reduction of NB by FeO is an exothermic reaction (10.8 kcal/mol). In disagreement with these data the B3LYP approach predicts this reaction

to be endothermic by 3.1 kcal/mol. Otherwise, the pure DFT approach such as BLYP is in good agreement with the experiment revealing that the reaction is exothermic by 13.3 kcal/mol. Such an accuracy of the pure DFT approach might be due to the fortunate compensation of the errors in predicting the (−NO)−O and (OFe)−O bondings.

As our study of the initial stage of the nitrobenzene−FeO interaction reveals, there is a nonbarrier one-electron transfer from the d shell of iron into the antibonding LUMO localized mostly on the nitro group of nitrobenzene. This transfer results in the formation of the open-shell electronic configuration of the NB−FeO intermediate with a pair of α and β electrons occupying the d_δ(Fe) and $\pi^*(-NO_2)$ orbitals in addition to the remaining unpaired four α electrons on the d(Fe) orbitals. An indicator of this state is the $\langle S^2 \rangle$ value being about 1.0 larger than its eigenvalue of 6.0 for the quintet. Thus, the adsorption of the nitro group on ferrous iron is accompanied by a nonbarrier oxidation of ferrous to ferric iron. The NB−FeO intermediate formed accordingly is quite stable as predicted by all approaches.

The barrier of the oxygen removal from the nitro group by FeO depends on the particular DFT approach (Table 4) and appears to be minimal (16.2 kcal/mol) for BLYP, which is believed to be the best in predicting the thermodynamics of the considered process. Since the obtained activation energy is much less than the energy of the interaction between NB and FeO in the precursor complex, then the reduction of nitro- to nitrosobenzene by FeO seems to be possible at the elevated temperatures.

Acknowledgment. This work was facilitated by the support of NSF EPSCOR Grant No. 300423-190200-21000 and ONR Grant No. N00014-98-1-0592 and by the support of the Army High Performance Computing Research Center under the auspices of the Department of the Army, Army Research Laboratory Cooperative Agreement No. DAAH04-95-2-0003/ Contract No. DAAH04-95-C-0008, the content of which does not necessarily reflect the position or the policy of the government, and no official endorsement should be inferred. We thank the Mississippi Center for Supercomputer Research for a generous allotment of computer time. I.Z. acknowledges financial support from a Council of Russian President grants (Scientific School Grant No. 1140.2003.3), the Dutch Science Foundation (in the collaborative Russian−Dutch Research Project No. 047-015 001-NOW), and the Siberian Branch of Russian Academy of Sciences (Grant No. 4.1.16).

References and Notes

(1) Zengel, H. G. *Chem. Ing.-Tech.* **1983**, *55*, 962.
(2) Maltha A.; Vanwermeskerken Sc.; Brunet, B.; Ponec, V. *J. Mol. Catal.* **1994**, *93*, 305.
(3) Klausen, J.; Troeber, S. P.; Haderlein, S. B.; Schwarzenbach R. P. *Environ. Sci. Technol.* **1995**, *29*, 2396.
(4) Bauschlicher, C. W., Jr.; Langhoff, S. R.; Partridge, H. In *Modern Electronic Structure Theory*; Yarkony, D. R., Ed.; World Scientific: London, 1995.
(5) Siegbahn, P. E. M. *Adv. Chem. Phys.* **1993**, *93*, 333.
(6) Becke, A. D. *J. Chem. Phys.* **1993**, *98*, 5648.
(7) Glukhovtsev, M. N.; Bach, R. D.; Nagel, C. J. *J. Phys. Chem. A* **1997**, *101*, 316.
(8) Gutsev, G. L.; Khanna, S. N.; Rao, B. K.; Jena, P. *J. Phys. Chem. A* **1999**, *103*, 5812.
(9) Becke, A. D. *Phys. Rev. A* **1998**, *38*, 3098.
(10) Perdew, J. P.; Wang, Y. *Phys. Rev. B* **1991**, *45*, 13244.
(11) Chertihin, G. V.; Wendy, S.; Yustein, J. T., Andrews, L.; Matthew, N.; Ricca, A.; Bauschlicher, C. W., Jr. *J. Phys. Chem.* **1996**, *100*, 5261.
(12) Perdew, J. P. *Phys. Rev. B* **1986**, *33*, 8822.
(13) Kellogg, C. B.; Irikura, K. K. *J. Phys. Chem. A* **1999**, *103*, 1150.
(14) Grafenstein, J.; Cremer, D. *Mol. Phys.* **2001**, *99*, 981.
(15) Schlegel, H. B. In *Geometry Optimization on Potential Energy Surfaces in Modern Electronic Structure Theory*; Yarkony, D. R., Ed.; World Scientific: Singapore, 1995.
(16) Frisch, M. J.; Trucks, G. W.; Schlegel, H. B.; Scuseria, G. E.; Robb, M. A.; Cheeseman, J. R.; Zakrzewski, V. G.; Montgomery, J. A.. Jr.; Stratmann, R. E.; Burant, J. C.; Dapprich, S.; Millam, J. M.; Daniels, A. D.; Kudin, K. N.; Strain, M. C.; Farkas, O.; Tomasi, J.; Barone, V.; Cossi, M.; Cammi, R.; Mennucci, B.; Pomelli, C.; Adamo, C.; Clifford, S.; Ochterski, J.; Petersson, G. A.; Ayala, P. Y.; Cui, Q.; Morokuma, K.; Malick, D. K.; Rabuck, A. D.; Raghavachari, K.; Foresman, J. B.; Cioslowski, J.; Ortiz, J. V.; Baboul, A. G.; Stefanov, B. B.; Liu, G.; Liashenko, A.; Piskorz, P.; Komaromi, I.; Gomperts, R.; Martin, R. L.; Fox, D. J.; Keith, T.; Al-Laham, M. A.; Peng, C. Y.; Nanayakkara, A.; Challacombe, M.; Gill, P. M. W.; Johnson, B.; Chen, W.; Wong, M. W.; Andres, J. L.; Gonzalez, C.; Head-Gordon, M.; Replogle, E. S.; Pople, J. A. *Gaussian 98*, Revision A.9; Gaussian, Inc.: Pittsburgh, PA, 1998.
(17) Wachters, A. J. H. *J. Chem. Phys.* **1970**, *52*, 1033.
(18) Hay, P. J. *J. Chem. Phys.* **1977**, *66*, 4377.
(19) Raghavachari, K.; Trucks, G. W. *J. Chem. Phys.* **1989**, *91*, 1062.
(20) Boys, S. F.; Bernard, F. *Mol. Phys.* **1970**, *19*, 553.
(21) Schaftenaar, G. CAOS/CAMM Center Nijmegen, Toernooiveld, Nijmegen, The Netherlands, 1991.
(22) Domenicano, A.; Schultz, G.; Hargittai, I.; Colapietro, M.; Portalone, G.; George, P.; Bock, C. W. *Struct. Chem.* **1990**, *1*, 107.
(23) *CRC Handbook of Chemistry and Physics*, 74th ed.; Lide, D. R., Ed.; CRC Press: Boca Raton, FL, 1993−1994.
(24) Desfrancois, C.; Periquet, V.; Lyapustina, S. A.; Lippa, T. P.; Robinson, D. W.; Bowen, K. H.; Nonaka, H.; Compton, *J. Chem. Phys.* **1999**, *111*, 4569.
(25) Allen, M. D.; Ziurys, L. M.; Brown, J. M. *Chem. Phys. Lett.* **1996**, *257*, 130.
(26) Bagus, P. S.; Preston, H. J. T. *J. Chem. Phys.* **1979**, *9*, 2986.
(27) Rollason, R. J.; Plane, J. M. C. *Phys. Chem. Chem. Phys.* **2000**, *2*, 2335.
(28) Cheung, A. S. C.; Gordon, R. M.; Merer, A. J. *J. Mol. Spectrosc.* **1981**, *87*, 289.
(29) Steimle, T. C.; Nachman, D. F.; Shirley, J. E.; Merer, A. J. *J. Chem. Phys.* **1989**, *90*, 5360.
(30) Andrews, L.; Chertihin, G. V.; Ricca, A.; Bauschlicher, C. W., Jr. *J. Am. Chem. Soc.* **1996**, *118*, 467.
(31) Plane, J. M. C.; Rollason, R. J. *Phys. Chem. Chem. Phys.* **1999**, *1*, 1843.
(32) Zilberberg, I.; Pelmenschikov, A.; McGrath, C. J.; Davis, W. M.; Leszczynska, D.; Leszczynski, J. *Int. J. Mol. Sci.* **2002**, *3*, 801.
(33) Wittbrodt, J. M.; Schegel, H. B. *J. Chem. Phys.* **1996**, *105*, 6574.
(34) Zilberberg, I.; Ruzankin, S. *Chem. Phys. Lett.*, to be submitted for publication.
(35) Löwdin, P.-O. *J. Appl. Phys. Suppl.* **1962**, *33*, 251.
(36) Rodriguez, J. H.; McCusker, J. K. *J. Chem. Phys.* **2002**, *116*, 6253.
(37) Kohn, W.; Becke, A. D.; Parr, R. G. *J. Phys. Chem.* **1996**, *100*, 12974.
(38) Becke, A. D. *J. Chem. Phys.* **2000**, *112*, 4020.
(39) Afeefy, H. Y.; Liebman, J. F.; Stein, S. E. Neutral Thermochemical Data. In *NIST Chemistry WebBook* (March 2003); Linstrom, P. J., Mallard, W. G., Eds.; NIST Standard Reference Database Number 69;, National Institute of Standards and Technology: Gaithersburg, MD, 2003 (http://webbook.nist.gov).
(40) Hildenbrand, D. L. *Chem. Phys. Lett.* **1975**, *34*, 352.
(41) Weinhold, F.; Carpenter, J. E. *The Structure of Small Molecules and Ions*; Plenum: New York, 1988; p 227.
(42) Kaibicheva, E. A.; Rudnyi, E. B.; Sidorov, L. N. *Russ. J. Phys. Chem.* **1992**, *66*, 1679.
(43) Murad, E. *J. Chem. Phys.* **1980**, *73*, 1381.
(44) Uzunova E. L.; Nikolov G. S.; Mikosch H. *J. Phys. Chem. A* **2002**, *106*, 4104.